



## Discover Generics

Cost-Effective CT & MRI Contrast Agents



FRESENIUS  
KABI

WATCH VIDEO

# AJNR

## **In Re: Characterization of Benign and Metastatic Vertebral Compression Fractures with Quantitative Diffusion MR Imaging**

Robert V. Mulkern and Richard B. Schwartz

*AJNR Am J Neuroradiol* 2003, 24 (7) 1489-1491

<http://www.ajnr.org/content/24/7/1489>

This information is current as  
of June 30, 2025.

# In Re: Characterization of Benign and Metastatic Vertebral Compression Fractures with Quantitative Diffusion MR Imaging

We enjoyed reading the recent article by Zhou et al (1) on the application of quantitative diffusion imaging to the differential diagnosis of benign versus metastatic vertebral compression fractures. This article and the accompanying editorial provided useful insights into both the clinical dilemma posed by this problem and the limitations of current MR imaging methodology in addressing it. As we see it, the major “talking point” from the article is that quantitative diffusion imaging improves upon the use of qualitative diffusion-weighted imaging by eliminating the confounding effects of “T2 shine-through.” Although this improvement on the use of diffusion-weighted imaging alone is appreciated, it is our concern that the article under consideration and the few previous works in this arena (2–4) have either ignored or failed to appreciate adequately the extent to which lipid signal intensity within vertebral marrow may contribute to quantitative measurements of the tissue diffusion coefficient. Indeed, the discussions in these articles regarding the differences between diffusion characteristics of benign versus metastatic vertebral compression fractures tend to focus on the same biophysical mechanisms used to describe diffusion characteristics in brain and brain abnormalities where, of course, any lipid component can be safely ignored. This is not so in vertebral marrow; we demonstrate in this letter how even a fairly small fraction of lipid within a voxel can drastically affect diffusion coefficient measurements.

Healthy vertebral marrow contains some 20–70% lipid (5–12) with, according to the early spectroscopic studies of De Bisschop et al (5), approximately 7% increase in fat percentage per decade of life. Thus, a voxel of healthy vertebral marrow will contain a substantial signal intensity component from lipid. With the infiltration of malignant tumor or a more benign edematous process, the lipid component of the proton signal intensity can be expected to diminish. In our opinion, however, complete replacement of the lipid component with water will represent only an extreme condition. Thus, the tendency to ignore the lipid contribution—for either qualitative interpretations of diffusion-weighted imaging (2–4) or quantitative tissue diffusion measurements (1) within vertebral marrow, particularly when fat saturation or selective water excitation is not included in the pulse sequence design (1–4)—is simply not appropriate.

To justify this opinion requires consideration of how the lipid signal intensity can be anticipated to affect quantitative tissue diffusion coefficient measurements in vertebral marrow. Here we rely on our own measurements of the lipid diffusion coefficient in human scalp *in vivo*, which revealed that the large, slowly diffusing triglyceride molecules have a low diffusion coefficient  $D_p$  of approximately  $0.05 \mu\text{m}^2/\text{ms}$  (13). Let us now assume for the sake of argument that the water tissue diffusion coefficient  $D_w$ , takes a value of  $1.9 \mu\text{m}^2/\text{ms}$  as reported by Zhou et al for metastatic fractures within vertebral marrow (1). Because water and lipid protons do not exchange, the overall decay of signal intensity with *b* factor will then be described by a biexponential function of the form

$$1) \quad S = W\exp(-bD_w) + F\exp(-bD_p),$$

where *W* and *F* are the apparent amplitudes of the water and fat protons, respectively. The term “apparent” is used, because *W* and *F* do not represent solely the respective water and fat proton densities, but also T1 and T2 weightings. These in turn depend on the specifics of the pulse sequence (echo and re-

etition times) in combination with the fat and water relaxation times for which there is an established literature (9–12). Letting  $F + W = 1$  for normalization purposes, simulations based on equation 1 were generated for both an extended *b* factor range up to  $3000 \text{ s/mm}^2$  and for the more limited range below  $300 \text{ s/mm}^2$  employed by Zhou et al and others to study diffusion in vertebral marrow (1–4). Semilog plots of *S* versus *b* factor are provided in Figure 1, where the different curves in each plot represent different fat fractions from 0.05 (+), 0.15 (o), 0.25 (\*), and 0.35 (–). Over the extended *b* factor range (top plot) the nonmonoexponential nature of equation 1 reveals itself quite clearly as a curvature over the extended *b* factor range. Over the more limited *b* factor range relevant to the current clinical studies (lower plot), the decays actually appear monoexponential, but with lower diffusion coefficients (smaller slopes) observed with increasing fat fraction. Closer analysis of the simulated slopes reveals a nearly linear decrease with fat fraction in the apparent diffusion coefficient  $D_{app}$ , in this low *b* factor range. Figure 2 shows how a “monoexponential”-based  $D_{app}$  would be measured by using four *b* factors of 5, 70, 135, and  $200 \text{ s/mm}^2$  as the fat fraction increases from 0.05

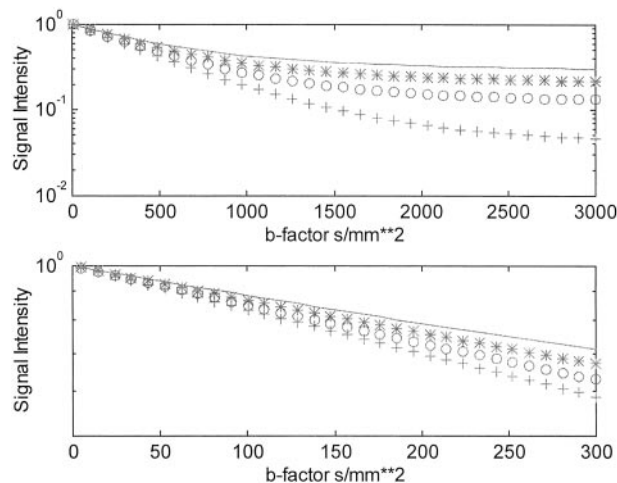


FIG 1. Simulated semilog plots of signal intensity versus *b* factor for marrow with varying fractions of fat for extended *b* factor range (top plots) and the limited *b* factor range used to date in most studies of vertebral marrow.

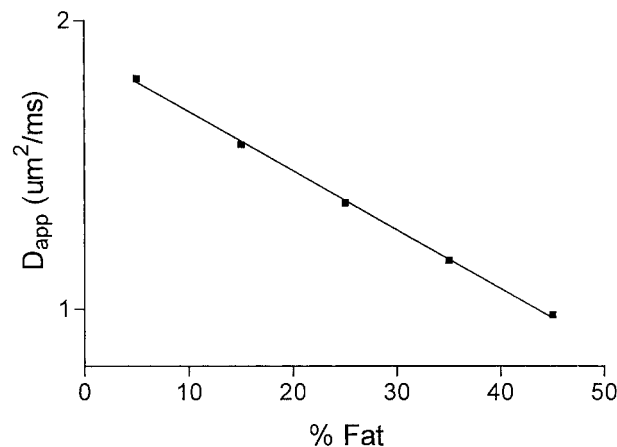


FIG 2. Plot of the apparent diffusion coefficient as a function of fat fraction in vertebral marrow when measured over the limited *b* factor range from 0 to  $200 \text{ s/mm}^2$ .

to 0.45. The correlation coefficients  $r^2$  for the linear regressions of the  $\ln(S)$  versus  $b$  factor fits used to obtain the  $D_{app}$  values were all above 0.999, effectively disguising the biexponential nature of the signal intensity decay due to the lipid component in this  $b$  factor range. Rather, the primary effect of increasing fat fraction in this low  $b$  factor range is to "artificially" lower  $D_{app}$ . The simulated results of Figure 2 are well represented by a linear regression fit as

$$2) \quad D_{app} = 1.88 - 0.02F,$$

with an  $r^2 > 0.99$ .

To conclude, we were concerned that Zhou et al and others who have begun to explore the potential of diffusion imaging in vertebral marrow have paid too little attention to the consequences of a lipid component on diffusion-weighted images and quantitative diffusion measurements. Figure 2 demonstrates how even small percentages of lipid within a voxel can dramatically affect the measured value of the diffusion coefficient. Because the non-echo-planar-based pulse sequences used to date for the vertebral marrow studies have not employed water selective or fat suppression methods (1–4), many of the forwarded interpretations of diffusion characteristics based on water specific models common to brain discussions seem premature.

Robert V. Mulkern

Richard B. Schwartz

Department of Radiology

Children's Hospital and Brigham and Women's Hospital

Harvard Medical School

Boston, Massachusetts

## References

1. Zhou XJ, Leeds NE, McKinnon GC, Kumar AJ. **Characterization of benign and metastatic vertebral compression fractures with quantitative diffusion MR imaging.** *AJNR Am J Neuroradiol* 2002; 23:165–170
2. Baur A, Stabler A, Bruning R, et al. **Diffusion-weighted MR imaging of bone marrow: differentiation of benign versus pathologic compression fractures.** *Radiology* 1998;207:349–356
3. Le Bihan DJ. **Differentiation of benign versus pathologic compression fractures with diffusion-weighted MR imaging: a closer step toward the "holy grail" of tissue characterization?** *Radiology* 1998; 207:305–307
4. Castillo M, Arbelaez A, Smith JK, Fisher LL. **Diffusion-weighted MR imaging offers no advantage over routine noncontrast MR imaging in the detection of vertebral metastases.** *AJNR Am J Neuroradiol* 2000;21:948–953
5. De Bisschop E, Luybaert R, Louis O, Osteux M. **Fat fraction of lumbar bone marrow using in vivo proton nuclear magnetic resonance spectroscopy.** *Bone* 1993;14:133–136
6. Mulkern RV, Meng J, Oshio K, et al. **Bone marrow characterization in the lumbar spine with inner volume spectroscopic CPMG imaging studies.** *J Magn Reson Imaging* 1994;4:585–589
7. Schellinger D, Lin CS, Fertikh D, et al. **Normal lumbar vertebrae: anatomic, age, and sex variance in subjects at proton MR spectroscopy—initial experience.** *Radiology* 2000;215:910–916
8. Jung CM, Kugel H, Schulte O, Heindel W. **Proton-MR-spectroscopy of vertebral bone marrow: normal age- and sex-related patterns.** *Radiologie* 2000;40:694–699
9. Kugel H, Jung C, Schulte O, Heindel W. **Age- and sex-specific differences in the 1H-spectrum of vertebral bone marrow.** *J Magn Reson Imaging* 2001;13:263–268
10. Traber F, Block W, Layer G, et al. **Determination of 1H relaxation times of water in human bone marrow by fat-suppressed turbo spin echo in comparison to MR spectroscopic methods.** *J Magn Reson Imaging* 1996;6:541–548
11. Masumoto A, Yonekura S, Haida M, et al. **Analysis of intramedullary cell density by MRI using the multiple spin-echo technique.** *Am J Hematol* 1997;55:134–138
12. Schick F, Bongers H, Jung WI, et al. **Proton relaxation times in human red bone marrow by volume selective magnetic resonance spectroscopy.** *Appl Magn Reson* 1992;3:947–963
13. Mulkern RV, Gudbjartsson H, Westin C-F, et al. **Multi-component apparent diffusion coefficients in human brain.** *NMR Biomed* 1999; 12:51–62

## Reply:

We thank Drs. Mulkern and Schwartz for their careful review of our article (1) and appreciate the opportunity to respond to their comments.

Drs. Mulkern and Schwartz expressed concern that our article, as well as several others on the same subject (2, 3), did not discuss the influence of lipid signal on diffusion-weighted images and on measurement of apparent diffusion coefficient (ADC) of vertebral bodies. On the basis of a two-compartment model that accounts for water and fat, they presented an empirical relationship between the ADC and the lipid fraction  $F$  (see Equation 2 of Drs. Mulkern and Schwartz's letter). This relationship indicates that the presence of lipid signal can contaminate the results in quantitative diffusion analysis, an aspect we did not consider in our article.

In *healthy* vertebral marrow, lipid content can be as high as 70% (4). Therefore, it is not negligible. For the two diseases we studied, however, the lipid fraction in the vertebral marrow can be considerably less. According to a study by Yuh et al (5), approximately 88% of vertebral metastasis cases exhibited *total* replacement of normal bone marrow. Similarly, edema in benign vertebral compression fractures can also replace normal marrow, resulting in substantially decreased lipid content in the lesion (6). In our study, the ADC values were calculated within a region of interest that contained *only* the vertebral lesion. Within the region of interest, the signal intensity of diffusion-weighted images arises predominantly from water, as evidenced by the T1-weighted, T2-weighted, and postcontrast T1-weighted images with or without fat suppression (Figs 1 and 2 in our article [1]). Therefore, we think it is appropriate to qualitatively discuss our results by using a water-only model.

Quantitatively, lipid signals within the region of interest can arise from either incomplete bone marrow replacement or the partial volume contamination. Thus, we agree with Drs. Mulkern and Schwartz that the possible presence of lipid should be considered. If we assume that the lipid fraction ranges from 0% to 20% among the regions of interest of the metastatic lesions in our study, equation 2 of Drs. Mulkern and Schwartz's letter indicates that the ADC value would vary between 1.88 and 1.48  $\text{mm}^2/\text{s}$ , with a standard deviation of 0.2  $\text{mm}^2/\text{s}$ . This standard deviation is not larger than what we observed in the study and is already contained in the error term ( $\pm 0.3 \text{ mm}^2/\text{s}$ ) we reported.

For normal vertebral bodies, wherein the lipid content cannot be neglected, we completely agree with Drs. Mulkern and Schwartz that a two-compartment model should be used to characterize the signals in diffusion-weighted images and determine the ADC values for water and fat separately. The primary focus for our article, however, was to present a possible way to differentiate benign from malignant vertebral compression fractures, not to provide a detailed account of the diffusion process in normal vertebral bodies.

In summary, Drs. Mulkern and Schwartz raised an important question in analyzing diffusion-weighted images and interpreting the ADC values in regions wherein both water and lipid signals are present. Within benign and malignant vertebral compression fractures, the impact of the lipid signal intensity is minimal. Thus, our explanation based on water diffusion remains valid and our conclusions unchanged. To extend quantitative diffusion imaging to other vertebral lesions, such as hemangiomas, we recommend that fat suppression techniques (eg, by using chemical suppression or spatial spectral excitation

radio-frequency pulses) be employed to reduce the effect of lipid signal intensity on ADC quantification.

Xiaohong Joe Zhou, Normal E. Leeds, and Ashok J. Kumar  
*M. D. Anderson Cancer Center  
 Houston, Texas*  
 Graeme C. McKinnon  
*Applied Science Laboratory  
 General Electric Medical Systems  
 Milwaukee, Wisconsin*

## References

1. Zhou XJ, Leeds NE, McKinnon GC, Kumar AJ. **Characterization of benign and metastatic vertebral compression fractures with quantitative diffusion MR imaging.** *AJNR Am J Neuroradiol* 2002; 23:165–170
2. Baur A, Stabler A, Bruning R, et al. **Diffusion-weighted MR imaging of bone marrow: differentiation of benign versus pathologic compression fractures.** *Radiology* 1998;207:349–356
3. Castillo M, Arbelaez A, Smith JK, Fisher LL. **Diffusion-weighted MR imaging offers no advantage over routine non-contrast MR imaging in the detection of vertebral metastases.** *AJNR Am J Neuroradiol* 2000;21:948–953
4. Kuchel PW, Coy A, Stilbs P. **NMR “diffusion-diffraction” of water revealing alignment of erythrocytes in a magnetic field and their dimensions and membrane transport characteristics.** *Magn Reson Med* 1997;37:637–643
5. Yuh WTC, Zachar CK, Barloon TJ, et al. **Vertebral compression fractures: distinction between benign and malignant cause with MR imaging.** *Radiology* 1989;172:215–218
6. Lafforgue P, Bayle O, Massonnat I, et al. **Magnetic-resonance imaging of osteoporotic and metastatic vertebral compression fractures in 60 patients.** *Ann Radiol (Paris)* 1991;34:157–166

## Subtraction Helical CT Angiography of Intra- and Extracranial Vessels: Technical Considerations and Preliminary Experience—Rediscovery of Matched Mask Bone Elimination?

We read with interest the article on subtraction angiography of the intra- and extracranial vessels by Jayakrishnan et al (1) in the March 2003 issue of the *AJNR*. From the authors' description, we surmise that their technique is a variant of a technique we have routinely used in our hospital for more than 4 years.

We would like to make the following comments. As in all subtraction techniques, two scans are made: one precontrast and the other postcontrast. We understand, however, that the first scan is used to identify the high attenuation structures (ie, bones and calcifications) and that this information is used to mask these structures in the postcontrast scan. If this assumption is correct, the term “subtraction” for this procedure is understandable—actually we used the same phrase in our first communication on this subject (2)—but it is incorrect. In subtraction, all the pixels in the volume of interest are involved, which leads to an overall deterioration of the image quality because of the increase of image noise, whereas in masking only the CT values of the high attenuation pixels are affected. This difference is especially important when the precontrast scan is made with a low dose. In an article on this subject (3), we explained this last method (matched mask bone elimination, or MMBE) and clearly demonstrated the advantages of masking over subtraction.

The use of a vacuum-type head holder to minimize movement is an interesting addition to this technique. The authors state that the use of this head holder *facilitates* image registration. From the information given in the rest of this article, we assume, however, that no registration is performed at all. In our experience, even the slightest movement of the patient in between the scans (in the order of 0.05 mm) may lead to a serious degradation in image quality. If (as we assume) the authors do

not use any registration, it would be interesting to investigate whether addition of such a registration step would produce an improvement in the quality of the processed images.

The use of image registration is completely feasible in a routine clinical setting. The authors give a mean postprocessing time for their procedure of slightly more than 8 minutes, by using software of the Omipro workstation of the CT-Twin CT-scanner. For comparison, the processing time of the MMBE software initially was in the order of 1 hour for one examination (3); because of improvements of the software and better performance of the hardware, this time has now been reduced to less than 10 minutes.

Hank W. Venema  
*Department of Radiology and  
 Medical Physics*  
 Gerard J. den Heeten  
*Department of Radiology  
 University of Amsterdam  
 Amsterdam, the Netherlands*

## References

1. Jayakrishnan VK, White PM, Aitken D, et al. **Subtraction helical CT angiography of intra- and extracranial vessels: technical considerations and preliminary experience.** *AJNR Am J Neuroradiol* 2003; 24:451–455
2. Venema HW, Hulsmans FJH, Van Lienden KP, den Heeten GJ. **CT angiography with 0.5 mm collimation of the circle of Willis and the intracranial part of the internal carotid arteries: maximum intensity projection (MIP) with matched mask subtraction.** *Radiology* 1999; 213(P):311
3. Venema HW, Hulsmans FJH, den Heeten GJ. **CT angiography of the circle of Willis and intracranial internal carotid arteries: maximum intensity projection with matched mask bone elimination—feasibility study.** *Radiology* 2001;218:893–898

## Reply:

We would like to thank Drs. Venema and den Heeten for their comments on our article (1).

We used the term “subtraction” in a manner consistent with the terminology used in the Omipro workstation to describe the process of subtracting a 3D mask from the 3D maximum intensity projection image. This does not mean a pixel-by-pixel subtraction, which will of course result in increased noise.

We did not use any image registration protocol in this study, because we often scan the head and neck and the degree of movement generated are probably more than what can be handled by such registration methods. It is for this reason we highlighted the use of the vacuum bag, which is a very good method of immobilization and is well tolerated by the patients. We agree with the Drs. Venema and den Heeten in that even the slightest movement between the scans can seriously degrade the image quality. To counter this, a further process of 3D mask expansion was sometimes employed, usually a one-pixel expansion was sufficient to reduce the artifacts to an acceptable level—a process similar to that used by Venema et al. (2).

V. K. Jayakrishnan  
*Department of Neuroradiology  
 The James Cook University Hospital  
 Middlesbrough  
 United Kingdom*

## References

1. Jayakrishnan VK, White PM, Aitken D, et al. **Subtraction helical CT angiography of intra and extracranial vessels: technical considerations and preliminary experience.** *AJNR Am J Neuroradiol* 2003; 24:451–455
2. Venema HW, Hulsmans FJH, den Heeten GJ. **CT angiography of the circle of Willis and intracranial internal carotid arteries: max-**



imum intensity projection with matched mask bone elimination—feasibility study. *Radiology* 2001;218:893–898

### Aortic Arch Origin of the Left External Carotid Artery

We read with interest the article by Horowitz et al (1) in the March 2003 issue of the *AJNR*. The authors described an aortic arch origin of the left external carotid artery associated with a type II preatlantal fetal anastomosis. They claim that their case is unique, because it shows a left external carotid artery originating from the aortic arch.

We would like to draw the authors' attention to the previously published reports of left external carotid arteries that have separate origins from the aortic arch. A search of the literature starting from 1968 revealed five cases of agenesis of left common carotid artery with separate origins of the left internal and external carotid arteries from the aortic arch. The condition was diagnosed by MR angiography of supraaortic vessels in a case by Cakirer et al (2), by using a combination of intraarterial angiography and duplex sonography in a case by Woodruff et al (3), and by using intraarterial angiography in three other cases by Bryan et al (4), Dahn et al (5), Rossitti et al (6).

The authors also claim that their case is unique in its association with a type II proatlantal intersegmental artery. Lie (7) reported that there were many congenital anomalies associated with separate origins of left internal and external carotid arteries from the aortic arch, including a cervical aortic arch, a double aortic arch, persistent trigeminal artery, and persistent proatlantal segmental artery in an angiographic study and review of congenital anomalies of the carotid arteries.

Sinan Cakirer and Ercan Karaarslan  
Istanbul Sisli Etfal Hospital

### References

1. Horowitz M, Bansal S, Dastur K. Aortic arch origin of the left external carotid artery and type II proatlantal fetal anastomosis. *AJNR Am J Neuroradiol* 2003;24:323–325
2. Cakirer S, Karaarslan E, Kayabali M, Rozanes I. Separate origins of the left internal and external carotid arteries from the aortic arch: MRA findings. *AJNR Am J Neuroradiol* 2002;23:1600–1602
3. Woodruff WW III, Strunsky VP, Brown NJ. Separate origins of the left internal and external carotid arteries directly from the aortic arch: duplex sonographic findings. *J Ultrasound Med* 1995;14:867–869
4. Bryan RN, Dreyer RG, Gee W. Separate origins of the left internal and external carotid arteries from the aorta. *AJR Am J Roentgenol* 1978;130:362–365
5. Dahn MS, Kaurich JD, Brown FR. Independent origins of the internal and external carotid arteries: a case report. *Angiology* 1999;50:755–760
6. Rossitti S, Raininko R. Absence of the common carotid artery in a patient with a persistent trigeminal artery variant. *Clin Radiol* 2001;56:79–81
7. Lie TA. Congenital anomalies of the carotid arteries: an angiographic study and a review of the literature. Amsterdam: Excerpta Medica Foundation; 1968;30–35

### Reply:

We greatly appreciate the information provided by Drs. Cakirer and Karaarslan regarding prior reports on aortic arch origins of the external carotid artery along with their association with proatlantal vessels. We apologize for incomplete review of the past literature. Once again, we have had it reinforced in our minds that there is rarely "something new under the sun." In retrospect, perhaps I should mind the valuable advice given to me by my mentor, Dr. Philip Purdy, several years ago, when he urged me never to say something is being reported for the first time, because one can be sure that this is not true.

Michael Horowitz  
University of Pittsburgh

### Diagnosis of Pseudosubarachnoid Hemorrhage

The recently published description of CT findings in pseudosubarachnoid hemorrhage (1) has, unfortunately, omitted to include neuropathologic correlation, despite the authors noting that subarachnoid hemorrhage was excluded on the basis of autopsy in three of the seven cases described. Despite this, the authors suggested that one possible cause for their findings—increased attenuation in the basal cisterns—was superficial vascular engorgement and dilatation (1). If this were true, enhancement following the administration of intravenous contrast medium could prove to be a useful method for confirming this diagnosis, as occurred in one of their cases. In, to my knowledge, the largest published series with this condition with detailed neuropathologic correlation (2), all five cases demonstrated increased attenuation in the basal cisterns, with (at autopsy) histologic evidence of congested and dilated subarachnoid and pial vessels in each, in addition to cerebral edema. Although Given and colleagues may be excused for omitting the latter article in their comprehensive literature review as the journal in which it was published was not—at that time—indexed by Medline, it indicates that the main cause for the CT appearances is vascular engorgement. Future studies should be directed toward determining whether head CT following the administration of intravenous contrast medium is a means of confirming this diagnosis when it is suspected clinically.

Morry Silberstein  
School of Medicine  
Monash University  
Melbourne, Australia

### References

1. Given CA, Burdette JH, Elster DA, Williams DW. Pseudo-subarachnoid hemorrhage: a potential pitfall associated with diffuse cerebral edema. *AJNR Am J Neuroradiol* 2003;24:254–256
2. Opeksin K, Silberstein M. False-positive diagnosis of subarachnoid haemorrhage on computed tomography scan. *J Clin Neurosci* 1998;5:382–386

### Reply:

As discussed in our publication (1), one of the contributing causes for the pseudosubarachnoid hemorrhage appearance seen with diffuse cerebral edema in engorgement of the superficial (pial) vasculature. We would like to thank Dr. Silberstein for bringing to our attention the publication by Opeksin and Silberstein (2), because it provides further support for vascular engorgement being a contributing factor in pseudosubarachnoid hemorrhage appearance. Contrasted studies may demonstrate enhancement of the subarachnoid space in such cases and prove useful for further evaluation in when the diagnosis is suspected.

Curtis A. Given II  
University of Kentucky Chandler Medical Center  
Lexington, Kentucky

### References

1. Given CA, Burdette JH, Elster DA, Williams DW. Pseudo-subarachnoid hemorrhage: a potential pitfall associated with diffuse cerebral edema. *AJNR Am J Neuroradiol* 2003;24:254–256
2. Opeksin K, Silberstein M. False-positive diagnosis of subarachnoid haemorrhage on computed tomography scan. *J Clin Neurosci* 1998;5:382–386

### Standardized Calculation of Brain Parenchymal Fraction: An Approach to Objective Assessment of Cerebral Atrophy

Various approaches to measure brain atrophy in MR imaging have been applied until now, including measures of ven-

tricular width and volume estimates of the whole brain or of limited regions of interest. Recently, Ge et al (1) proposed a semiautomated segmentation algorithm calculating fractional gray matter (GM) and white matter (WM) volumes from volumetric MR imaging data sets that were normalized to total intracranial volume.

Ge et al demonstrated a marked age dependency of GM and WM fractional volumes. If one combines the values of fractional GM and WM volumes into the ratio of brain parenchymal volume to total intracranial volume, the resulting measure is the brain parenchymal fraction (BPF). This measure, first introduced by Rudick et al (2), has been validated as a useful quantitative MR imaging marker for investigating destructive processes ongoing in relapsing-remitting multiple sclerosis and has been applied for intraindividual longitudinal monitoring (eg, in controlled therapy trials [3]).

Such standardized measures, however, have yet to enter into general clinical practice. Although many of previous approaches for quantifying brain atrophy suffered from major drawbacks—availability of (costly) software, reproducibility of measures, and comparability with previously published results—standardized protocols offer a possible solution for quantitative assessment of atrophy instead of visual inspection alone. BPF may also be calculated in a highly automated and observer-independent way by using the algorithms implemented in Statistical Parametric Mapping software (4; SPM2b, Wellcome Department of Cognitive Neurology, London, [http://www.fil.ion.ucl.ac.uk/spm/spm2b.html]). Because SPM, in all its versions from 1994 until 2002, is freely available to the scientific public and has meanwhile gained a general acceptance for application to clinical studies, there now exists a fast, widely available, and validated method to generate an accurate measure of global brain atrophy in terms of BPF values that may be included in every single report of an individual MR imaging scan in routine diagnostics for neurodegenerative disease.

Discriminating between shrinkage of the brain considered to be appropriate for the patients' age and atrophy because of neurodegenerative disease may thus turn from an inherently subjective diagnosis to a rational diagnosis based on an objectively quantified measure. Prerequisite, however, for correct interpretation of BPF values from a single patient is the presence of BPF values from an age- and sex-matched normal database, as age and sex effects have been demonstrated previously (1, 5). Because of its standardized calculation, BPF

values from normal controls can easily be shared with the neuroimaging community.

Freimut D. Juengling  
Department of Radiology,  
Neuroradiology and Nuclear Medicine  
Inselspital and University Hospital  
of Bern  
Bern, Switzerland  
Jan Kassubek  
Department of Neurology  
University of Ulm  
Ulm, Germany

## References

1. Ge Y, Grossman RI, Babb JS, et al. **Age-related total gray matter and white matter changes in normal adult brain. Part I. Volumetric MR imaging analysis.** *AJNR Am J Neuroradiol* 2002;23:1327–1333
2. Rudick RA, Fisher E, Lee JC, et al. **Brain atrophy in relapsing multiple sclerosis: relationship to relapses, EDSS, and treatment with interferon beta-1a.** *Mult Scler* 2000;6:365–372
3. Fisher E, Rudick RA, Cutter G, et al. **Relationship between brain atrophy and disability: an 8-year follow-up study of multiple sclerosis patients.** *Mult Scler* 2000;6:373–377
4. Chard DT, Parker GJ, Griffin CM, et al. **The reproducibility and sensitivity of brain tissue volume measurements derived from an SPM-based segmentation methodology.** *J Magn Reson Imaging* 2002;15:259–267
5. Chard DT, Griffin CM, Parker GJ, et al. **Brain atrophy in clinically early relapsing-remitting multiple sclerosis.** *Brain* 2002;125:327–337

## Reply:

I don't have much more comments on this letter except one thing mentioned in the letter. The brain parenchymal fraction was not first introduced by Rudick et al. This was first introduced by Micheal D. Phillips et al. in the article: Comparison of T2 lesion volume and magnetization transfer ratio histogram analysis and of atrophy and measures of lesion burden in patients with multiple sclerosis. *AJNR* 1998;19:1055–1060. In that article they called it as "percentage of brain parenchyma."

Yulin Ge  
Department of Radiology  
New York University  
New York, NY

## Erratum

In the article **Curved-Surface Projection: An Alternative Method for Visualizing Functional MR Imaging Results** by Scheef L et al. *AJNR* 24: 1045–1048, June/July 2003, the authors would like to acknowledge a mistake in the list of authors as printed. The author list which reads as follows: Lukas Scheef, Klaus Hoenig, Horst Urbach, Hans Schild and Roy Koenig is corrected as **Lukas Scheef, Klaus Hoenig, Horst Urbach, Christiane Kuhl, Hans Schild, and Roy Koenig.**